Parameterisation of Frequency Domain Models of Power Electronic Interfaced Renewable Energy Sources and VSC-HVDC for Harmonic Studies

BERND WEISE, GENEVIEVE LIETZ

DIgSILENT GmbH, Germany

Abstract:

This paper summarises typical frequency domain models of power electronic (PE) interfaced renewable energy sources (RES), such as wind turbines or photovoltaic (PV) inverters, and of voltage-sourced converters (VSC) of high voltage direct current (HVDC) for the analysis of harmonics emissions. The focus of the paper is on the parameterisation of these models in practical applications. Dependencies of the harmonic spectra on VSC operating points (power bins) are considered, and discussion of the practical challenges for a correct model parameterisation is provided. Special attention is given to the phase angles of harmonic currents and voltages. Phase angles of interharmonics are also discussed. The paper highlights methods to parameterise the inner sources of Norton and Thevenin equivalents, based on measurements at the terminals of the device in the field and at test benches while considering the influence of the network impedance. Possibilities to parameterise models based on incomplete measurements are discussed, and limitations shown. Drawbacks of insufficient models and of assumptions in the parameterisation (in cases of incomplete measurements) are explained.

Keywords:

Harmonics analysis, frequency domain models, power electronic interfaced renewable energy sources (RES), high voltage direct current (HVDC), voltage-sourced converter (VSC), Norton equivalent, Thevenin equivalent, phase angle, prevailing angle, interharmonics

1. Introduction

For the analysis of harmonic emissions of power electronic (PE) interfaced renewable energy sources (RES), such as wind turbines or photovoltaic (PV) inverters, and of high voltage direct current (HVDC) converters, their behaviour is usually assumed to correlate with ideal harmonic current sources. Measurement approaches and existing certification procedures often follow this assumption (e.g. [1, 2]). Practical experiences over recent years have highlighted however, that voltage-sourced converters (VSC) interact with the grid and therefore cannot be treated as ideal harmonic current sources [3, 4, 5]. Enhanced measurement procedures [6] and modelling approaches [4, 5, 7, 8] have been proposed. The draft IEC technical report 61400-21-3 suggests modelling wind turbines as Norton or Thevenin equivalents [8]. The parameterisation of these equivalents based on field measurements requires information about the phase angles of harmonic currents and voltages, which are not usually disclosed in harmonics measurements reports according to IEC 61400-21 [1]. Suggested procedures to determine phase angles from measurements of time-varying harmonics exist [9, 10]. The usage of the prevailing angle is seen as a practical solution in technical guidelines [6, 10].

This paper is organised as follows: Section 2 introduces the above-mentioned models in detail. Section 3 describes the parameterisation of the models as follows: Subsection 3.1 and 3.2 introduce the basic means to parameterise the models. Subsection 3.3 focuses on phase angles, Subsection 3.4 on dependencies on operating points. Subsection 3.5 addresses parameterisation in cases of incomplete measurements. Conclusions are drawn in Section 4.

2. Frequency Domain Models of PE Interfaced RES and VSC-HVDC

The ideal current source, depicted in Fig. 1, is the simplest model to represent harmonic injections. This model is commonly used and in many cases provides a good representation of harmonics injected by line-commutated converters (LCC) such as thyristor converters of HVDC systems [11].

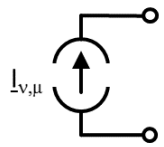

Figure 1 Ideal current source

For PE interfaced RES and VSC-HVDC systems, and for devices with VSCs in general, a Thevenin or Norton equivalent (see Fig. 2) better represents the harmonic behaviour of such devices (the term ‘harmonics’ used here includes integer order harmonics and interharmonics unless stated otherwise). These equivalents are characterised by their open-circuit voltage and short-circuit current, as shown in Eq. 1 and 2. The inner voltage source of the Thevenin equivalent equals the open-circuit voltage, while the inner current source of the

Paper submitted on April 30, 2017. Paper accepted on May 15, 2017.

Paper presented in Session 7-1 of ICEE 2017 in Weihai, China on July 7, 2017.
Reprint version revised by authors after ICEE 2017; text revisions are marked in green.

Norton equivalent equals the short-circuit current. In case of a two-level VSC, the impedance represents the series reactor, the filters and in some cases the machine or converter transformer. In case of a modular multi-level converter (MMC), which is usually used for VSC-HVDC, the impedance mainly represents the arm reactors (half the value of one arm reactor). If the controller transfer function is considered and represented by the impedance, the equivalent can be used not only for harmonics analysis, but also for impedance-based stability analysis [12]. If the device behaves linearly, i.e. the impedance or admittance does not depend on the voltage or current, the Thevenin and Norton equivalents are equivalent to each other, as indicated by Eq. 3. The inner sources can be easily calculated from each other, see Eq. 4 and 5.

$$\underline{Z}(f) = \frac{\underline{U}_{\nu,\mu,open-circuit}}{\underline{I}_{\nu,\mu,short-circuit}} = \frac{\underline{U}_{\nu,\mu}}{\underline{I}_{\nu,\mu,short-circuit}} \quad (1)$$

$$\underline{Y}(f) = \frac{\underline{I}_{\nu,\mu,short-circuit}}{\underline{U}_{\nu,\mu,open-circuit}} = \frac{\underline{I}_{\nu,\mu}}{\underline{U}_{\nu,\mu,open-circuit}} \quad (2)$$

$$\underline{Y}(f) = 1/\underline{Z}(f) \Leftrightarrow \underline{Z}(f) = 1/\underline{Y}(f) \quad (3)$$

$$\underline{I}_{\nu,\mu} = \frac{\underline{U}_{\nu,\mu}}{\underline{Z}(f)} = \underline{U}_{\nu,\mu} \cdot \underline{Y}(f) \quad (4)$$

$$\underline{U}_{\nu,\mu} = \frac{\underline{I}_{\nu,\mu}}{\underline{Y}(f)} = \underline{I}_{\nu,\mu} \cdot \underline{Z}(f) \quad (5)$$

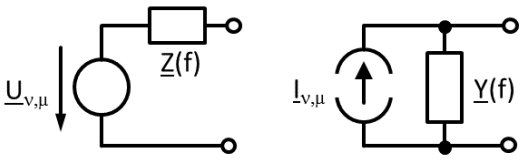

Figure 2 Thevenin equivalent (left) and Norton equivalent (right)

In order to use the same impedance representation in the Norton and Thevenin equivalents, it is useful to express the Norton equivalent with a parallel impedance Z(f) instead of a parallel admittance Y(f), see Eq. 6 and Fig. 3. This way, the Thevenin equivalent can be used for the Norton equivalent as well. This is the approach taken in the commercially available network analysis software DIgSILENT PowerFactory.

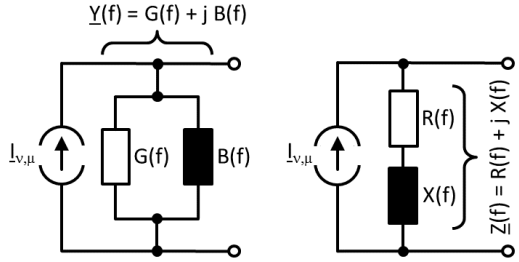

Figure 3 Norton equivalent with admittance (left), and with impedance (right)

It should be noted that both the real and imaginary parts of the admittance appear in the real part of the impedance (Eq. 7) as well as in the imaginary part of the impedance (Eq. 8).

$$\underline{Z}(f) = R(f) + j \cdot X(f) = \frac{1}{\underline{Y}(f)} = \frac{1}{G(f)+j \cdot B(f)} \quad (6)$$

$$R(f) = \frac{G(f)}{G^2(f)+B^2(f)} \quad (7)$$

$$X(f) = \frac{-B(f)}{G^2(f)+B^2(f)} \quad (8)$$

Fig. 4 shows the possible interaction of PE interfaced RES or HVDC VSC with existing background harmonics, i.e. with a harmonic voltage distortion pre-existing in the grid regardless the connected RES or HVDC VSC. The background harmonic voltages feed harmonic current components flowing into the admittance of the Norton equivalent, as shown in Eq. 9. The injected harmonic current components of the RES or HVDC VSC depend on the impedances given in Eq. 10. The resulting current that can be measured is written in Eq. 11.

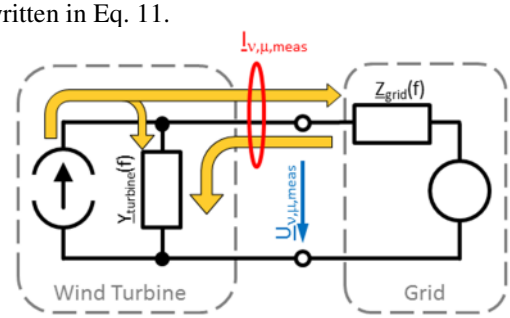

Figure 4 Norton equivalent illustrating potential interactions with background harmonics from the grid [3]

$$\underline{I}_{\nu,\mu,Grid\rightarrow Turb.} = \frac{\underline{U}_{\nu,\mu,Grid}}{\underline{Z}_{Grid}(f)+\underline{Z}_{Turb.}(f)} \quad (9)$$

$$\underline{I}_{\nu,\mu,Turb.\rightarrow Grid} = \underline{I}_{\nu,\mu,Turb.} \cdot \left(1 - \frac{\underline{Z}_{Grid}(f)}{\underline{Z}_{Grid}(f)+\underline{Z}_{Turb.}(f)}\right) \quad (10)$$

$$\underline{I}_{\nu,\mu,meas} = \underline{I}_{\nu,\mu,Turb.\rightarrow Grid} - \underline{I}_{\nu,\mu,Grid\rightarrow Turb.} \quad (11)$$

The effective use of a Thevenin equivalent to model a type 4 wind turbine was demonstrated in [13] as follows:

- The harmonic emissions from the converter are represented as several Thevenin equivalent circuits at relevant harmonic or interharmonic frequencies.
- The equivalent impedances in the model can be used to represent the physical components (smoothing reactor, harmonic filters) and the converter closed loop control, thereby representing the interaction between the converter and background harmonics.
- The inner voltage sources in the model represent harmonic disturbances caused by the switching of the power electronic valves.

Paper submitted on April 30, 2017. Paper accepted on May 15, 2017.
Paper presented in Session 7-1 of ICEE 2017 in Weihai, China on July 7, 2017.
Reprint version revised by authors after ICEE 2017; text revisions are marked in green.

In the case of VSC-HVDC with MMC, the equivalent impedance should be modelled as accurately as possible, because it represents exclusively the converter impedance (as no ac filters are present) and will determine any background harmonic amplification caused by resonance between the network impedance and the converter equivalent impedance.

3. Parameterisation of Frequency Domain Models

This section describes the means to parameterise the models introduced in Section 2.

3.1 Ideal Current Source

The ideal current source model is very easy to parameterise, under the assumption that the current injected by the source is independent from any outer condition, i.e. independent from the grid impedance or background harmonic voltage distortion at the terminal. The value of the harmonic current source is equal to the harmonic current measured at the source terminal.

Measurement reports nowadays usually list the harmonic current magnitudes in percent, based on the nominal apparent current of the device [1, 10]. Care has to be taken with the definition of the nominal apparent current, which is used for the conversion of the measured data. The nominal apparent current is either the current at nominal apparent power and nominal voltage (Eq. 12), or it is the current at nominal active power (i.e. apparent power with unity power factor) and nominal voltage (Eq. 13). The latter approach is usually used for measurements and in measurement reports.

Using the current at nominal apparent power for the model while the measurement report uses the current at unity power factor errs on the side of caution but leads to a slight overestimation of the injected harmonic currents as indicated by Eq. 14. The recalculation of the harmonic current for the precise representation is given in Eq. 15.

$$I_{base(Sn)}[A] = \frac{S_n[kVA]}{\sqrt{3}\cdot U_n[kV]} \quad (12)$$

$$I_{base(Pn)}[A] = \frac{S_n\cdot\cos(\varphi_n)}{\sqrt{3}\cdot U_n} = \frac{P_n\cdot\cos(0)}{\sqrt{3}\cdot U_n} \quad (13)$$

$$\begin{aligned} I_{\nu,\mu}[A] &= I_{\nu,\mu}[\%_{Pn}]\cdot I_{base(Sn)}[A] \\ &\geq I_{\nu,\mu}[\%_{Pn}]\cdot I_{base(Pn)}[A] \end{aligned} \quad (14)$$

$$\begin{aligned} I_{\nu,\mu}[A] &= I_{\nu,\mu}[\%_{Pn}]\cdot\frac{P_n}{S_n}\cdot I_{base(Sn)}[A] \\ &= I_{\nu,\mu}[\%_{Sn}]\cdot I_{base(Sn)}[A] \end{aligned} \quad (15)$$

3.2 Norton and Thevenin Equivalents

As the Norton and Thevenin equivalents consist of an inner source and an impedance (or admittance), both must be parameterised.

3.2.1 Parameterisation of the Impedance

As previously mentioned, the impedance mainly represents series reactors or arm reactors, filters and in some cases the machine or converter transformer. The controller transfer function can be considered and represented by the impedance as well [8], which is particularly important for impedance-based stability analysis [12].

The equivalent impedance can be determined in a theoretical analytical way by deriving the frequency characteristics from the device's internal impedances (e.g. passive filters) and from the controller transfer functions (small signal representation) as indicated in [4, 5, 7]. It is also possible to measure the impedance as seen from the device terminal, as described in [14], if the inner source is negligible in the frequency range of interest. In a three-phase system the sequences (pos., neg., zero sequence) have to be considered and measurements taken accordingly. The equivalent impedance can be different in the individual sequences, as described in [4, 5, 7] and indicated in [8].

If dynamic models for EMT simulation exist, which represent the behaviour with sufficient precision in the frequency range of interest, the frequency characteristic of the impedance can be determined via EMT simulations which emulate the above-mentioned tests. The latter approach is advantageous especially for operating points which are difficult to measure [14]. Validation of the simulation models against available measurements is recommended.

An example template for a possible representation of the frequency-dependent equivalent impedance in tabular format (i.e. look-up table) is provided in [8].

3.2.2 Parameterisation of the Inner Source

To parameterise the inner source of the Norton or Thevenin equivalent, both harmonic currents and voltages have to be measured. It is not sufficient to only use the magnitudes. Magnitudes and phase angles have to be taken into account. This means that harmonic currents and voltages have to be measured simultaneously and phase-correct.

If the complex impedance of the equivalent is known, the inner source can be parameterised as shown in Eq. 16 (Thevenin equivalent) or Eq. 17

Paper submitted on April 30, 2017. Paper accepted on May 15, 2017.
Paper presented in Session 7-1 of ICEE 2017 in Weihai, China on July 7, 2017.
Reprint version revised by authors after ICEE 2017; text revisions are marked in green.

(Norton equivalent).

$$\underline{U}_{\nu,\mu} = \underline{U}_{\nu,\mu,meas} + \underline{Z}(f) \cdot \underline{I}_{\nu,\mu,meas} \quad (16)$$

$$\underline{I}_{\nu,\mu} = \underline{I}_{\nu,\mu,meas} + \frac{\underline{U}_{\nu,\mu,meas}}{\underline{Z}(f)} \quad (17)$$

If the measurements are performed in a laboratory or at a test bench, for which the frequency-dependent impedance of the whole set-up is known and no other harmonic source exists besides the device under test (DUT), the inner source of the Thevenin equivalent (Eq. 18) or Norton equivalent (Eq. 19) can be parameterised without measurement of the harmonic voltage. It should be noted that this is not possible for measurements in the field, for which the frequency-dependency of the grid impedance and the background harmonics sources which are present during the measurement are usually not known.

$$\underline{U}_{\nu,\mu} = \underline{I}_{\nu,\mu,meas} \cdot \left(\underline{Z}_{DUT}(f) + \underline{Z}_{TestBench}(f)\right) \quad (18)$$

$$\underline{I}_{\nu,\mu} = \underline{I}_{\nu,\mu,meas} \cdot \left(1 + \frac{\underline{Z}_{TestBench}(f)}{\underline{Z}_{DUT}(f)}\right) \quad (19)$$

Example templates for a possible representation of the inner source of the Norton and Thevenin equivalents in a tabular format (i.e. look-up tables) are provided in [8].

3.3 Phase Angles

Phase angles of harmonic currents and voltages have to be considered if the Norton or Thevenin equivalent is parameterised, as described in Section 3.2. In the following subsections considerations referring to phase angles which are important for harmonic studies are listed.

It should be noted that even if the phase angles have to be considered for calculation of the values for the inner sources, it would still be possible to use only the magnitude of the resulting complex number for the inner source in the model. This applies a magnitude only (instead of a complex number) for the inner sources in Fig. 1, 2 and 3. By following the latter approach, a summation law (for example as defined in [1, 10, 15]) would be needed to investigate the harmonic propagation of several harmonic sources in a harmonic study. This is preferable if it is not certain that the contributions of the harmonic sources are synchronised to their local angle reference points at the fundamental frequency (i.e. if the PAR is small; see Section 3.3.3), and for interharmonics in general. If the harmonic sources show a synchronised behaviour related to the local angle reference points, consideration of the phase angles in the harmonic models and using a complex harmonic load flow calculation in harmonic studies will provide more precise results and should be favoured.

3.3.1 Reference Point for Phase Angles

Measurements and complex network calculations usually use different reference points for phase angles. As soon as harmonic sources of more than one device type are considered in the harmonic study, this fact has to be taken into account and the phase angles of the sources parameterised correctly.

In measurements the zero crossing of the fundamental frequency voltage is usually taken as the reference point for all angles, because it is easy to detect. Fig. 5 shows the time domain voltages and currents and the corresponding angles as defined in [6, 10]. The zero crossing as reference point refers to a sine function. Currents and voltages can be expressed as written in Eq. 20 to 23.

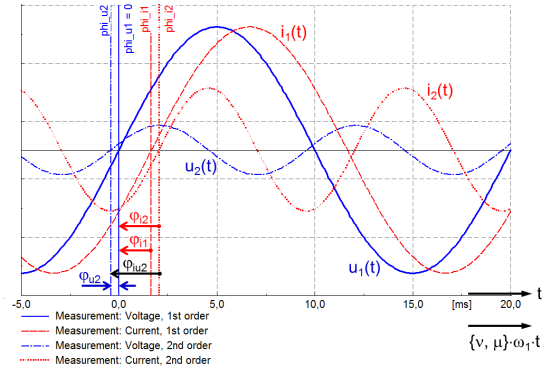

Figure 5 Angles resulting from measurements depicted as corresponding time curves

$$u_1(t) = \sqrt{2} \cdot U_1 \cdot \sin\left(\omega_1 \cdot t + \varphi_{u,1}^{sin}\right) = \sqrt{2} \cdot U_1 \cdot \sin(\omega_1 \cdot t) \quad \text{with } \varphi_{u,1}^{sin} = 0 \quad (20)$$

$$i_1(t) = \sqrt{2} \cdot I_1 \cdot \sin\left(\omega_1 \cdot t + \varphi_{i,1}^{sin}\right) \quad (21)$$

$$u_\nu(t) = \sqrt{2} \cdot U_\nu \cdot \sin\left(\omega_\nu \cdot t + \varphi_{u,\nu}^{sin}\right) \quad (22)$$

$$i_\nu(t) = \sqrt{2} \cdot I_\nu \cdot \sin\left(\omega_\nu \cdot t + \varphi_{i,\nu}^{sin}\right) \quad (23)$$

The real part of the complex number used in network calculations represents a cosine function, as indicated by the Euler function in Eq. 24 (with time function) and Eq. 25 (for steady-state calculations without time function). Therefore, in network calculations, the peak of the sinusoidal waveform is usually taken to be the reference point, referring to the cosine function.

$$e^{j(\omega t+\varphi)} = \cos(\omega t + \varphi) + j \cdot \sin(\omega t + \varphi) \quad (24)$$

$$e^{j\varphi} = \cos(\varphi) + j \cdot \sin(\varphi) \quad (25)$$

To represent the time curves of Fig. 5 by cosine functions instead of sine functions, Eqs. 20 - 23 should be rewritten as Eqs. 26 - 29 with a shift of the angle by -90 degrees (= -π/2) to keep the same reference point in time.

$$u_1(t) = \sqrt{2} \cdot U_1 \cdot \cos\left(\omega_1 \cdot t - \frac{\pi}{2}\right) \quad (26)$$

$$i_1(t) = \sqrt{2} \cdot I_1 \cdot \cos\left(\omega_1 \cdot t + \varphi_{i,1}^{sin} - \frac{\pi}{2}\right) \quad (27)$$

$$u_\nu(t) = \sqrt{2} \cdot U_\nu \cdot \cos\left(\omega_\nu \cdot t + \varphi_{u,\nu}^{sin} - \frac{\pi}{2}\right) \quad (28)$$

$$i_\nu(t) = \sqrt{2} \cdot I_\nu \cdot \cos\left(\omega_\nu \cdot t + \varphi_{i,\nu}^{sin} - \frac{\pi}{2}\right) \quad (29)$$

Changing to the reference point (t = 0) from the zero crossing to the peak of the sinusoidal waveform changes the equations without any loss of general information [16]. Note that the time point t = 0 is an arbitrarily defined point and can be changed without loss of general information. Fig. 6 shows the corresponding angles. Eqs. 30 - 33 provide the mathematical representation [16].

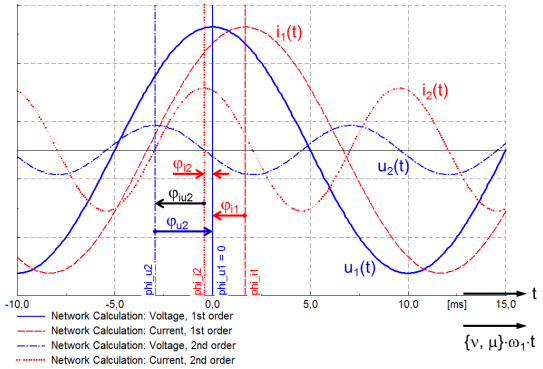

Figure 6 Angles in complex network calculation depicted as corresponding time curves

$$u_1(t) = \sqrt{2} \cdot U_1 \cdot \cos\left(\omega_1 \cdot t + \varphi_{u,1}^{cos}\right) \quad (30)$$
$$= \sqrt{2} \cdot U_1 \cdot \cos(\omega_1 \cdot t) \quad \text{with} \quad \varphi_{u,1}^{cos} = 0$$

$$i_1(t) = \sqrt{2} \cdot I_1 \cdot \cos\left(\omega_1 \cdot t + \varphi_{i,1}^{sin} + (1-1) \cdot \frac{\pi}{2}\right)$$
$$= \sqrt{2} \cdot I_1 \cdot \cos\left(\omega_1 \cdot t + \varphi_{i,1}^{cos}\right) \quad (31)$$

$$u_\nu(t) = \sqrt{2} \cdot U_\nu \cdot \cos\left(\omega_\nu t + \varphi_{u,\nu}^{sin} + (\nu-1) \cdot \frac{\pi}{2}\right) \quad (32)$$

$$i_\nu(t) = \sqrt{2} \cdot I_\nu \cdot \cos\left(\omega_\nu t + \varphi_{i,\nu}^{sin} + (\nu-1) \cdot \frac{\pi}{2}\right) \quad (33)$$

The phase angles of the harmonics can be rewritten as shown in Eq. 34 [16], leading to a simplified representation in the time functions, Eq. 35 and 36. Eq. 34 shows the re-calculation of the angles from measurements (corresponding to sine function) to network calculation input (corresponding to cosine function).

$$\varphi_\nu^{cos} = \varphi_\nu^{sin} + (\nu-1) \cdot \frac{\pi}{2} \quad (34)$$

$$u_\nu(t) = \sqrt{2} \cdot U_\nu \cdot \cos\left(\omega_\nu \cdot t + \varphi_{u,\nu}^{cos}\right) \quad (35)$$

$$i_\nu(t) = \sqrt{2} \cdot I_\nu \cdot \cos\left(\omega_\nu \cdot t + \varphi_{i,\nu}^{cos}\right) \quad (36)$$

As the harmonic currents are often synchronised with the current of the fundamental frequency (for LCC this is always the case; for VSC it depends on the effect which causes the harmonic and on the pulse pattern of IGBT switching), it makes sense to use an angle for the harmonic currents which is not related to the fundamental frequency voltage, but to the fundamental frequency current. Eq. 36 can be rewritten as Eq. 37; Eq. 38 shows the angle representation. The harmonic current phase angle deviation is described by Eq. 39, which would be the input to harmonic current sources in PowerFactory, if phase angles are taken from measurement reports. It should be noted that the phase angle of the fundamental frequency current is the same, independently of whether the zero crossing (measurement) or the peak of the sinusoidal waveform (complex number representation in calculation) is used as the reference point.

$$i_\nu(t) \quad (37)$$
$$= \sqrt{2} \cdot I_\nu \cdot \cos\left(\omega_\nu \cdot t + h \cdot \varphi_{i,1} + \Delta\varphi_{i,\nu}^{cos}\right)$$
$$= \sqrt{2} \cdot I_\nu \cdot \cos\left(h \cdot \left(\omega_1 \cdot t + \varphi_{i,1}\right) + \Delta\varphi_{i,\nu}^{cos}\right)$$

$$\Delta\varphi_{i,\nu}^{cos} = \varphi_{i,\nu}^{cos} - h \cdot \varphi_{i,1} \quad (38)$$

$$\Delta\varphi_{i,\nu}^{cos} = \varphi_{i,\nu}^{sin} + (\nu-1) \cdot \frac{\pi}{2} - h \cdot \varphi_{i,1} \quad (39)$$

3.3.2 Interharmonics

The accurate consideration of interharmonics, i.e. non-integer harmonic orders, presents particular challenges [17, 18]. For interharmonics it is inappropriate to use a phase angle which is related to the fundamental frequency, because this causes the angle to change with every period of the fundamental frequency, as the period of an interharmonic is not an integer multiple of the fundamental frequency period.

In such cases, it is appropriate to use angles for interharmonics as well, however the information of interest is the phase angle between current and voltage of the same frequency (Eq. 40), i.e. of the same interharmonic. In other words, the voltage of the same interharmonic is the reference for the angle of the interharmonic current. It should be noted that the angle used for the displacement factor cos(φ) is defined in the opposite direction, because the conjugated complex current is used in the power equations.

$$\varphi_{iu,\mu} = \varphi_{i,\mu} - \varphi_{u,\mu} \quad (40)$$

In addition to the phase angle, the sequence in which the interharmonic voltages and currents exist (i.e. positive, negative or zero sequence) is of interest [18]. Therefore, analysis of the angles of the phases B and C referring to the interharmonic voltage of phase A of the same frequency as shown in Eqs. 41 - 43 is of importance.

$$\varphi_{uA,\mu}^{refA} = 0 \quad (41)$$

$$\varphi_{uB,\mu}^{refA} = \varphi_{uB,\mu} - \varphi_{uA,\mu} \quad (42)$$

$$\varphi_{uC,\mu}^{refA} = \varphi_{uC,\mu} - \varphi_{uA,\mu} \quad (43)$$

It should be noted that Eqs. 40 - 43 are valid if the same reference point (regardless if it is the zero crossing or the peak of the sinusoidal waveform) is used within each period of the fundamental frequency (see Section 3.3.1).

3.3.3 Prevailing Angle

A harmonic measurement contains a number of discrete Fourier transform (DFT) windows. The result for each individual DFT window can vary from the others. Hence an aggregation of the measurement results is needed.

For the magnitude of the harmonic voltage or current the mean value of all DFT windows is taken as aggregation as shown in Eq. 44. The variable C represents either voltage or current. N is the number of aggregated DFT windows.

$$C_{\{\nu,\mu\}} = \frac{1}{N} \cdot \sum_{n=1}^{N} \left| \underline{C}_{\{\nu,\mu\},n} \right| \quad (44)$$

For the phase angles, a simple mean value would not reflect results correctly (for example the mean value of 10 degrees and 350 degrees would yield 180 degrees, which is the opposite angle direction). IEC 61400-21-1 [10] and FGW guideline TR3 [6] suggest the prevailing angle as an average of the angle, which is defined by Eq. 45 [8, 10]. An alternative formulation is provided in Eq. 46, which ensures that the range of the prevailing angle is always within -π to +π (-180° to +180°).

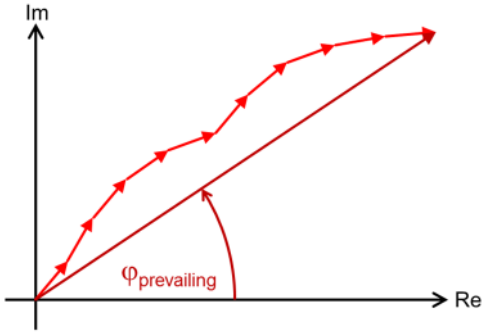

Figure 7 Prevailing Angle

The prevailing angle represents the direction of the complex vector sum of all phasors of the N DFT windows, as indicated in Fig. 7. If the individual phasors have a similar direction, the prevailing angle gives their common direction. If the individual phasors have large deviations in their directions, the prevailing angle will tend to be random. The Prevailing Angle Ratio (PAR) is needed for information regarding the quality of the result. The PAR is the length of the vector sum of the N phasors, in relation to the arithmetic sum of the magnitudes, as defined in Eq. 47.

$$\varphi_{\{\nu,\mu\},prevailing} = \quad (45)$$
$$= \begin{cases} atan\left(\frac{\sum_{n=1}^{N} Im\{\underline{C}_{\{\nu,\mu\},n}\}}{\sum_{n=1}^{N} Re\{\underline{C}_{\{\nu,\mu\},n}\}}\right) & if \quad \sum_{n=1}^{N} Re\{\underline{C}_{\{\nu,\mu\},n}\} \geq 0 \\ \pi + atan\left(\frac{\sum_{n=1}^{N} Im\{\underline{C}_{\{\nu,\mu\},n}\}}{\sum_{n=1}^{N} Re\{\underline{C}_{\{\nu,\mu\},n}\}}\right) & if \quad \sum_{n=1}^{N} Re\{\underline{C}_{\{\nu,\mu\},n}\} < 0 \end{cases}$$

$$\varphi_{\{\nu,\mu\},prevailing} = \quad (46)$$
$$= sign\left(\sum_{n=1}^{N} Im\{\underline{C}_{\{\nu,\mu\},n}\}\right) \cdot acos\left(\frac{\sum_{n=1}^{N} Re\{\underline{C}_{\{\nu,\mu\},n}\}}{\left|\sum_{n=1}^{N} \underline{C}_{\{\nu,\mu\},n}\right|}\right)$$
$$= \begin{cases} acos\left(\frac{\sum_{n=1}^{N} Re\{\underline{C}_{\{\nu,\mu\},n}\}}{\left|\sum_{n=1}^{N} \underline{C}_{\{\nu,\mu\},n}\right|}\right) & if \quad \sum_{n=1}^{N} Im\{\underline{C}_{\{\nu,\mu\},n}\} \geq 0 \\ -acos\left(\frac{\sum_{n=1}^{N} Re\{\underline{C}_{\{\nu,\mu\},n}\}}{\left|\sum_{n=1}^{N} \underline{C}_{\{\nu,\mu\},n}\right|}\right) & if \quad \sum_{n=1}^{N} Im\{\underline{C}_{\{\nu,\mu\},n}\} < 0 \end{cases}$$

$$PAR = \frac{\left|\sum_{n=1}^{N} \underline{C}_{\{\nu,\mu\},n}\right|}{\sum_{n=1}^{N} \left|\underline{C}_{\{\nu,\mu\},n}\right|} = \frac{\left|\sum_{n=1}^{N} (a_{\{\nu,\mu\},n} + j \cdot b_{\{\nu,\mu\},n})\right|}{\sum_{n=1}^{N} \left|(a_{\{\nu,\mu\},n} + j \cdot b_{\{\nu,\mu\},n})\right|} \quad (47)$$

If the PAR is close to unity, the phase angle does not vary significantly [10] and can be considered for harmonic studies. A PAR of 0.9 or higher indicates a very stable phase angle [6]. The phase angle is considered as random if the PAR is smaller than 0.3 [10].

The prevailing angle and PAR can be applied to interharmonics as well. These should be applied to the angles related to the voltage of the same interharmonic (as described in Section 3.3.2), because angles of interharmonics related to the fundamental frequency quantities are random by nature and would always result in a very small PAR.

3.4 Dependencies of Harmonic Spectra on Operating Points

The harmonic spectrum of a VSC or a PE interfaced RES can vary depending on the operating point of the device. Therefore IEC 61400-21 requires harmonics measurements at 11 power bins (0%, 10%, 20%, …, 90%, 100%) [1, 10].

3.4.1 Ideal Current Source

To achieve the worst-case conditions for the harmonic analysis, the maximum values of all power bins must be selected for each harmonic (and interharmonic) for the parameterisation of the ideal current source model (i.e. resulting in maximum current injection), if only magnitudes are

considered in the harmonic study. It should be noted that the resulting worst-case spectrum does not reflect a particular power bin, but can comprise a mix of different power bins at different orders (or frequencies).

If the harmonic study is carried out using a complex harmonic load flow calculation and the sources are considered with phase angles, the worst-case condition at the node of interest not only depends on the magnitudes of the individual sources, but also on their phase angles. See Section 3.4.2 for details.

3.4.2 Norton and Thevenin Equivalents

If the frequency-dependent impedance of the Norton or Thevenin equivalent is the same for each power bin, the same approach as for the ideal current source model also applies to the Norton or Thevenin equivalent. However, from the measurements of currents and voltages at the terminal, the values for the inner source have to be calculated first for each power bin, as explained in Section 3.2. Subsequently, the maximum value (max. magnitude) of the inner source can be selected per power bin to achieve the worst-case spectrum. It should be noted that this approach is only possible if only magnitudes are considered for parameterisation of the sources, but phase angles are neglected, and summation laws are used for the summation of harmonic currents and voltages at the point of connection or point of common coupling (i.e. the node of interest) in the harmonic study. If the harmonic study is carried out using a complex harmonic load flow calculation and the sources are considered with phase angles, the worst-case condition at the node of interest does not only depend on the magnitudes of the individual sources, but also on their phase angles. This also applies to the ideal current source model. Therefore, if phase angles of sources are considered and the harmonic sources in the network are not all of the same device type, each spectrum of power bin has to be considered in the harmonic study. This means that the harmonic load flow calculation must be repeated for all power bins in order to not miss any worst-case scenario.

Assuming that the frequency-dependent impedance of the Norton or Thevenin equivalent may be different for each power bin (this may apply if components of the device are non-linear or if the controller transfer function changes for different operating points), for parameterisation of the Norton or Thevenin equivalent, the worst-case conditions are very difficult to select. This is because a worst case can be caused by maximum current injection, by injection of different sources with the same phase angle (not necessarily with maximum magnitudes, if injections of max. magnitudes differ in phase angles and therefore result in a lower superposition), or by a resonance of the impedance of the Norton or Thevenin equivalent (inner impedance) with the grid impedance (outer impedance). This means that if the impedance varies with power bins, the related spectrum of the inner source as well as the frequency-dependent inner impedance must be considered for each power bin in a harmonic study. Again, the harmonic load flow calculation must be repeated for all power bins so as not to miss any worst-case scenario if the Norton or Thevenin equivalent is used.

In PowerFactory, network model variations can be used for the representation of the individual input data referring to power bins. Scripting or automatic task execution is recommended to carry out all necessary harmonic load flow calculations, either in a loop or even in parallel, distributed on several cores of the computer [19].

3.5 Parameterisation of Models based on Incomplete Measurements

As described in Section 3.2, measurement of the harmonic current and voltage (both with magnitude and angle) is needed to parameterise the Norton or Thevenin equivalent, unless the frequency-dependent impedance of the entire set-up is known. If these measurements are not performed and only the harmonic current magnitudes are known, the models cannot be parameterised sufficiently.

Taking the harmonic current measured at the terminal of the device as the inner current of the Norton equivalent or as short-circuit current for parameterising the inner source of the Thevenin equivalent following Eq. 5 (or using Eq. 16 but entering the harmonic voltage at the terminal as zero), will in most cases lead to an underestimation of the harmonic injection in the harmonic study. This is because the magnitude of the inner source must be larger in order to achieve the measured harmonic currents at the terminal.

If no harmonic voltage measurement is available, a rough estimation is possible by reproducing the impedances of the measurement set-up as accurately as possible for the parameterisation. This should be done using the same assumptions for the frequency characteristics of the impedances as will be used later in the harmonic study. With these assumptions, Eq. 18 or 19 can be used to estimate the values of the inner sources.

4. Conclusions

This paper provides a detailed discussion of the Norton and Thevenin equivalent for representation of PE interfaced RES and VSC of HVDC system in harmonic studies. Correct parameterisation of the models is crucial for their use in harmonic studies. As the complex harmonic currents and voltages (or impedances of the whole test set-up) are needed for the parameterisation, consideration of the phase angles is very important. Procedures to evaluate phase angles from measurements and to transform them in a correct way for use in network calculations are described in detail. The formulas needed for parameterisation of the models are provided.

References

[1] IEC 61400-21, Wind turbines – Part 21: Measurement and assessment of power quality characteristics of grid connected wind turbines. Edition 2.0, 2008 (IEC 61400-21:2008)

[2] FGW TR8, Technical Guidelines for Power Generating Units – Part 8: Certification of the Electrical Characteristics of Power Generating Units and Farms in the Medium-, High- and Highest-voltage Grids, Rev. 8, Dec. 2016, FGW e.V., Germany

[3] F. Santjer, B. Weise, T. Pausch, J. Brombach: Aspects for Improvement of Measurement and Assessment Procedures of Harmonic Emission of Wind Power Plants, DEWEK 2015, Bremen, Germany, 19-20 May 2015

[4] M. Cespedes, J. Sun: Modeling and Mitigation of Harmonic Resonance Between Wind Turbines and the Grid, IEEE Energy Conversion Congress and Exposition, 2011

[5] J. Sun: Modeling and Mitigation of Harmonics and Harmonic Resonance Involving Wind Inverters, 12th Wind Integration Workshop (International Workshop on Large-Scale Integration of Wind Power into Power Systems as well as on Transmission Networks for Offshore Wind Power Plants), London, 2013

[6] FGW TR3, Technical Guidelines for Power Generating Units – Part 3: Determination of electrical characteristics of power generating units connected to MV, HV and EHV grids. Rev. 24, March 2016, FGW e.V., Germany

[7] M. Cespedes, J. Sun: Impedance Modeling and Analysis of Grid-Connected Voltage-Source Converters, IEEE Trans. on Power Electronics, Vol. 29, No. 3, March 2014, pp. 1254-1261

[8] IEC Technical Report 61400-21-3, Wind turbine harmonic model and its application, Draft Version, 2016 (IEC DC 61400-21-3 TR)

[9] K. Malekian, A. Gürlek, W. Schufft: Analysis and Modeling of Time-Varying Harmonics in Frequency Domain, 9th International Conference on Compatibility and Power Electronics, Portugal, 2015

[10] IEC 61400-21-1, Wind energy generation systems - Part 21-1: Measurement and assessment of electrical characteristics - Wind turbines, Committee Draft for Vote (CDV), 2017 (IEC CDV 61400-21-1:2017)

[11] Cigré WG 14.39 Brochure 139: Guide to the Specification and Design Evaluation of AC Filters for HVDC Systems, April 1999

[12] J. Sun: Impedance-based stability criterion for grid-connected inverters, IEEE Trans. on Power Electronics, Vol. 26, No. 11, Nov. 2011, pp. 3075-3078

[13] L. Shuai, Ł. H. Kocewiak, K. H. Jensen: Application of Type 4 Wind Turbine Harmonic Model for Wind Power Plant Harmonic Study, 15th Wind Integration Workshop (Intl. Workshop on Large-Scale Integration of Wind Power into Power Systems…), Vienna, 2016

[14] M. Aberhard, M. Meyer, C. Courtois: EN 50388-2 – der neue Teil 2: Stabilität und Harmonische, Elektrische Bahnen, Vol. 112, No. 10, 2014, pp. 574-581

[15] IEC Technical Report 61000-3-6: Electro-magnetic compatibility (EMC) – Part 3-6: Limits – Assessment of emission limits for the connection of distorting installations to MV, HV and EHV power systems, Edition 2.0, 2008-02 (IEC/TR 61000-3-6:2008)

[16] M. H.J. Bollen, I. Y.H. Gu: Signal Processing of Power Quality Disturbances, IEEE Press, Wiley-Interscience, 2006, ISBN 978-0-471-73168-9

[17] IEEE Task Force on Harmonics Modeling and Simulation (A. Testa, et al.): Interharmonics: Theory and Modeling, IEEE Trans. on Power Delivery, Vol. 22, No. 4, 2007, pp. 2335-2348

[18] D. Zhang, W. Xu, Y. Liu: On the Phase Sequence Characteristics of Interharmonics, IEEE Trans. on Power Delivery, Vol. 20, No. 4, Oct. 2005, pp. 2563-2569

[19] DIgSILENT PowerFactory 2017 User Manual, DIgSILENT GmbH, Germany, 2017

Authors' brief introduction and contact information:

Dipl.-Ing. Bernd Weise (e-mail address: b.weise@digsilent.de) obtained his Dipl.-Ing. Degree (diploma degree) in electrical engineering from the Technical University of Berlin, Germany, in 2002. In 2007 he joined DIgSILENT GmbH, Gomaringen, Germany, as an application and consulting engineer. In 2013 he became manager of the "Application Engineering" department. Since 2016 he leads the "Power Generation and Conversion" department, which is responsible for application engineering and consulting in the field

of electric power generation and power conversion systems within DIgSILENT. Mr. Weise represents DIgSILENT in working groups of FGW e.V. (encourage-society for wind energy and other renewable energies), Germany, and is chairman of a working group on Harmonic Models within FGW e.V.

Dr. Genevieve Lietz (e-mail address: g.lietz@digsilent.de) obtained the Bachelor of Engineering (Hons) from the School of Electrical and Computer Systems Engineering at RMIT University, Melbourne, Australia, in 2001. She obtained the PhD from the Faculty of Engineering at the University of Melbourne in 2007. From 2006-2007 she worked as a power systems consulting engineer at DIgSILENT Pacific, Melbourne, Australia, and since 2007 works as a power systems engineer and software developer at DIgSILENT GmbH, Gomaringen, Germany. Her primary areas of interest are harmonic analysis and modelling, and EMT cable/line modelling. She is a member of the CIGRÉ Joint Working Group C4/B4.38 on Network Modelling for Harmonic Studies.